Hindawi
Journal of Sensors
Volume 2022, Article ID 8701988, 12 pages
https://doi.org/10.1155/2022/8701988

Research Article

Monitoring Evolution of Coastline along Mto Tamamba Delta in Kenya North Coast Using Satellite Images

D. N. Aketch,[1] **C. O. Mito**,[1] **and G. Laneve**[2]

[1]*Department of Physics, University of Nairobi, P. O. Box, 30197-00100 Nairobi, Kenya*
[2]*Sapienza University of Rome, Piazzale Aldo Moro, 5, 00185 Roma, Italy*

Correspondence should be addressed to D. N. Aketch; aketchnewton@yahoo.com

Received 14 June 2022; Revised 10 August 2022; Accepted 9 September 2022; Published 15 October 2022

Academic Editor: Kathiravan Srinivasan

Coastal zones are the epicenter of economic activities in most developing countries in the world hence are bound to change. With advancement in technology, monitoring degradation of coastal zones using remote sensing (RS) and geographic information system (GIS) has become a critical subject for scientific research. RS refers to the process of detecting and monitoring the physical characteristics of an area by measuring its reflected and emitted radiation at a distance (typically from satellite or aircraft) while GIS is a system that creates, manages, analyzes, and maps all types of data. This paper reports an evolving Kenyan coastline over the past three decades using RS and GIS. Literature on chronological evolution and its impacts along this coastline is scanty and it is therefore envisaged that this work will instigate more enquiry into factors that were involved in landscape formation along the Kenyan coast. Prior reports indicate that research work done along this coastline were by field survey. We report a prograding beach on Mto Tamamba delta as displayed by multispectral Landsat imagery. The marine ecosystems, riparian communities and tourism industry are facing a major threat. The finding establishes hydrodynamic effects and human influence as key contributors of this menace. This study is aimed at detecting the coastline change using multispectral Landsat images from the years 1990 to 2021. For this purpose, coastlines belonging to these years were drawn numerically with the aid of GIS and RS on ENVI 5.3 software. We utilized maximum likelihood algorithm to categorize the images, and employed a time series methodology on classified endmembers to infer the presence of erosion and accretion. Using the image subset technique, areas prone to erosion and accretion within the coastal datum were identified and cut. The patterns of spatiotemporal trend of these endmembers were effectively employed to corroborate these findings. Change in distribution of endmembers over the 31 years' period was assessed using thematic change technique; an approach not previously applied in this study area. From the classified Mto Tamamba image, the pixel coverage area for each endmember was extracted. Validation using field campaign data gave an overall accuracy of 84% and kappa coefficient of 0.799. Taking into account that, the traditional methods of monitoring land degradation over a large area are time consuming and expensive; remote sensing data used in this study has offered alternatively cheap, consistent, reliable and retrievable data.

1. Introduction

One of the most important uses of remote sensing in Earth science is the detection of changes in coastline morphology. Tidal fluctuations, waves, and longshore current are listed as main processes leading to shoreline changes [1]. These processes not only play an important role in sediment budget but also modify the coastline leading to evolution. Coastline can be defined as dynamic boundary line between land and sea [2]. The change in coastline is brought about by physical as well as anthropogenic processes along the shore and has a large impact on the immediate environment and its riparian communities. Detection of coastline change plays an important role in coastal management, hazard notification, erection of coastal structures, sediment budget and modeling of coastal morphodynamics [3, 4].

Climate change, earth crust movement, wind and wave regimes are among the morphological factors influencing the shape of coastlines [5]. These morphological factors escalate the evolution process. According to field campaigns,

this study identifies erosion of silt down steam as well as hydrodynamic influence on seabed as key contributors of this evolution. The retreat and accretion rate are determined by sediment budget from seabed as well as from land. The excess supply of sediment due to water dynamics leads to accretion while a deficit gives chance for water to recede into the land. Coastal erosion is often accompanied by shoreward recession of coastline and always leads to loss of land area [6] consequently, aquatic animals as well as tourism industry face environmental threat. [7, 8].

Researchers worldwide have used several methods in assessing coastal vulnerability. This includes remote sensing, geographical information system, dynamic assessment tools and vulnerability indices among others [9]. Coastline vulnerability is defined as the potential for natural hazards on the coast to inflict damage [10, 11]. Changes in the global climate have increased the frequency of natural disasters such as storm surges, tsunamis, and cyclones, wreaking havoc on coastlines [12]. The tsunami of December 2004 and the Thane cyclone of 2011 both wreaked havoc on the coastlines of Puducherry and Tamil Nadu, causing massive human and economic losses [13]. The destruction created by the aforementioned catastrophes necessitates vulnerability assessment in order to identify the factors that cause the menace. On a global scale, the most often utilized methods in the research of coastal erosion and accretion are remote sensing (RS) and geographic information systems (GIS). For example, [6] used RS and GIS to manage coastal erosion in Southeast India. [14] used six remote sensing images to determine shoreline change in China's Pearl River Estuary from 1986 to 2011.[15] employed a variety of satellite images, including MSS, TM, and ETM+, to determine coastline erosion. Rosetta promontory lost 113.8 m per year between 1984 and 1991 [16]. Moreover, [17] showed that satellite data can be used to assess the effect of shoreline protections. [18] studied the long-term shoreline oscillations of the Cauvery Delta at Poompuhar, Tharangambadi, and Nagapattinam using satellite images, and they also physically observed these three locations with the help of reference pillars and compared the results with the images. [19] determined coastline change in the Aksehir and Eber lakes in southwest Turkey using different remote-sensing methods on satellite images during different periods. [20] used remote sensing to identify and evaluate hot spots of shoreline changes to determine the pattern of shoreline changes along the Turkish coast of the Black Sea.

The Kenyan coast, like other coastlines across the world, has been subjected to natural and human-caused coastline erosion and accretion. Many research work on coastal erosion in this region are based on field survey. [21] points out that anthropic activities, such as mangrove exploitation at the edge of the mangrove forest (Shirazi-Funzi lagoon), expose the shoreline to wave current, allowing erosion to occur. In fact, [22] states that erosion related to unwise agricultural practice, clearance of land for settlement, dredging of seabed and deforestation are prevalent at the Kenyan coast. Because the loss of fertile soil is generally followed by a drop in food production, coastal erosion is a severe problem. Physical surveys, which are of course, more expensive and time demanding, are currently used to identify the afflicted areas. As a result, this study explores the use of more acceptable and less complex methods of gathering data, and satellite remote sensing provides an effective remedy. Research work done by [23] along the coastline reveals that, Malindi Bay receives high terrigenous sediment load amounting to 5.7×10^6 ton·yr−1. Coastal erosion and sedimentation carried by River Sabaki affect not only the beaches but also the coral of Malindi area [24]. Coastal erosion is severe in a number of sandy beach areas such as North and South of Mombasa and Malindi – Mambrui area, while in areas around Mambrui village, rapid accretion is occurring (KMFRI, 2003). Before 1976 Malindi was experiencing loss of land, but from 1976 to date, the beach at Malindi has prograded by about 500 m [25]. Coastal erosion is also prevalent along the cliffs beaches at Kanamai, Shanzu, Ivwetine, Nyali, Likoni, Black Cliff Point, and Tiwi (P. A. [26]).

The goal of this study is to use satellite images (Landsat) to track the evolution of Kenya's coastline. Remote sensors via satellite have the capability of monitoring land surface changes and degradation on different scales. The ability of satellite sensors to distinguish spectral signature of various elements (water, soil, vegetation) has made it possible to accomplish the objective of this research. We combine RS and GIS approaches to monitor silt distribution along the Mto Tamamba delta (from 1990 to 2021) and provide conclusions based on time series data. This study was motivated by the evident need to control the threat of coastal erosion to coastal communities in Kenya and the whole world.

2. Materials and Methods

2.1. Description of the Study Area. We studied a coastal strip within Kenya facing Indian Ocean. The Kenyan coastal zone has a total shoreline length of over 480 km (Intergovernmental Oceanographic Commission,1994). This study identifies Mto Tamamba delta in Marereni location (Kenya North coast) along the coastline, as the most affected area. Mto Tamamba region extents from about $2^0$45' S to 2^0 48'S and has a total shoreline length of approximately 3.8 km. It borders Tana River to its North, Kanangoni township to the West, Marereni township to the South and Indian ocean to the East. Mto Tamamba is located in Marereni location, Magarini Sub-County in Kilifi County. This sub-county is a host to many salt manufacturing industries that supply salts to entire Republic of Kenya. The study area is approximately 12 square Kilometers. The natives are mainly Mijikenda people whose economic activities include fishing, coconut farming, goat rearing and trade. The most dominant feature along the shore in the study area is mangrove forests. Figure 1 shows location of Mto Tamamba area on coastal map. While Figure 2 shows selected RGB landsat data from Mto Tamamba delta. Coastal climate is tropical humid and is influenced by the monsoon wind which is characterized by two distinct rainy seasons. Long rainy season is between March to May and coincides with south-east monsoon wind whereas short rains which is from October to December corresponds to northeast monsoon wind [27]. Annual average rainfall along the coast varies from 500-

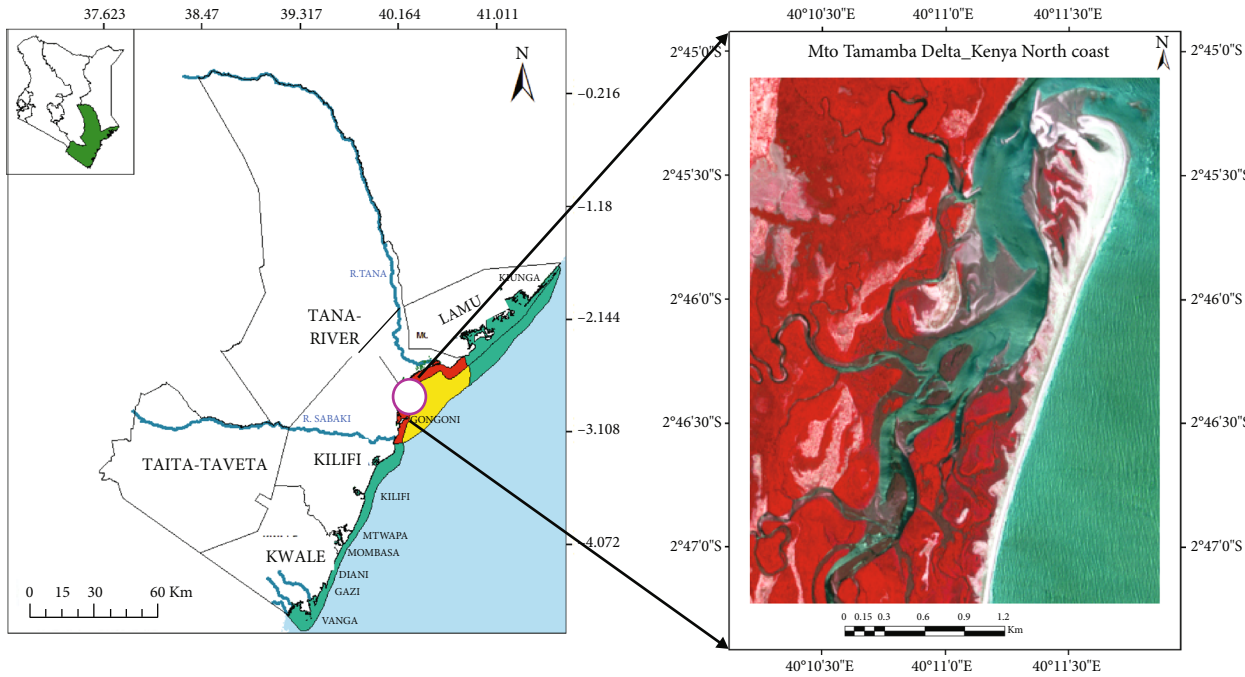

Figure 1: Map showing the satellite image for the study area (adapted from (Latawiec & Agol [28]), KMFRI).

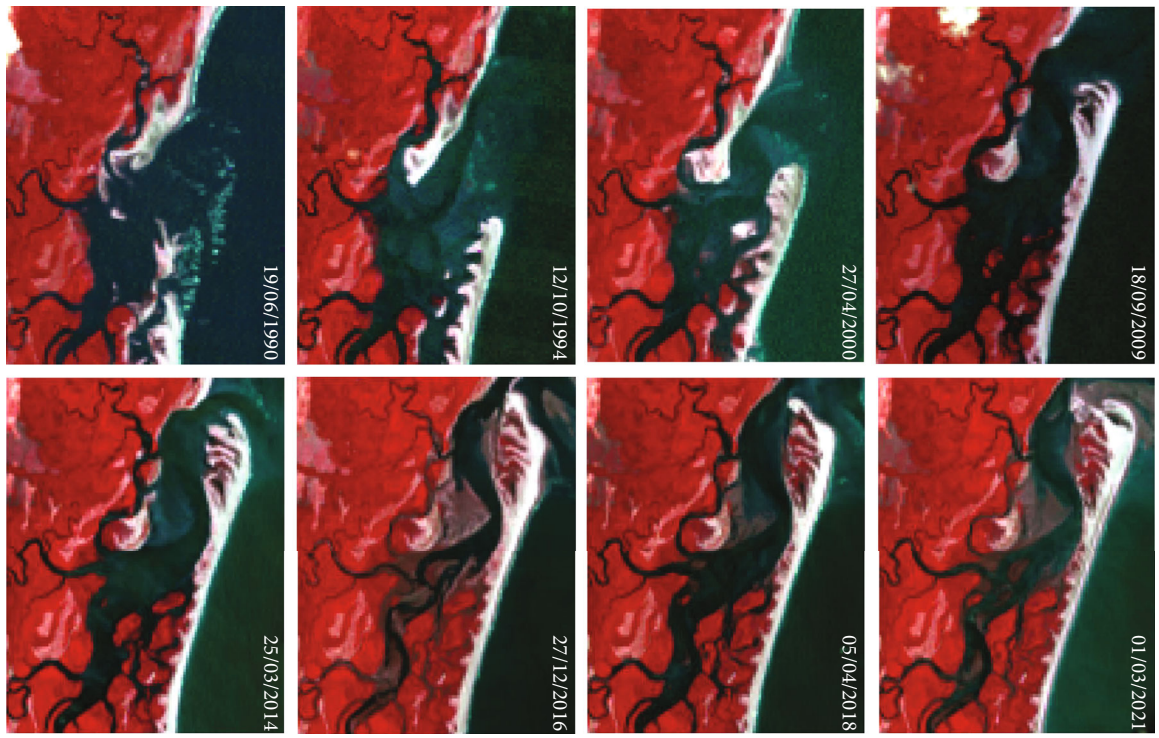

Figure 2: Selected Landsat RGB images showing temporal variation of an evolving Kenyan coastline (Source: https://usgs.gov/).

900 mm per year on north coast to 1500-1600 mm per year on south coast (UNEP, 1998). The mean minimum and maximum temperature at Kenyan coast range between 24°C and 30°C.

2.2. Remote Sensing Data. To achieve the objective of this study, several Landsat images covering the area of interest and period of interest were downloaded from https://earthexplorer.usgs.gov/. The TM, ETM+, and OLI from Landsat for period 1990 to 2021 were used. These images were selected on the basis of spatial and spectral resolution with cloud cover threshold below 5% put into consideration. The sensor specifications for images used in this study are listed in Table 1. Table 2 shows acquisition dates of images

Table 1: Satellite images and their sensor specifications used in this study (Source: https://Earthexplorer.usgs.gov/).

Specification	Landsat 5	Landsat 7	Landsat 8
Sensor	Thematic mapper (TM)	Enhanced thematic mapper plus (ETM +)	Operational land imager (OLI)
Spectral resolution (bands)	7	8	11
Spatial resolution	Band 1 to 5 and 7 (30 m)-band 6 (120 m)	Band 1 to 5 and 7 (30 m)-band 6 (60 m)-band 8 (15 m)	Band 1to 7 and 9 (30 m)-band 8 (15 m)-band 10 & 11 (100 m)
Temporal resolution (days)	16	16	16
Acquisition date	1990	2000	2014 to 2021
Coordinate system/datum	UTM/WGS 84		
Zone	37S		

Table 2: Details of satellite data used, their acquisition dates and resolution.

Satellite and sensor	Date of image acquisition	Path/raw	Band used	Spatial resolution
Landsat 5 TM	1990-06-19	166/062	Visible & NIR	30 m
Landsat 5 TM	1994-10-12	166/062	Visible & NIR	30 m
Landsat 7 ETM+	2000-04-27	166/062	Visible & NIR	30 m
Landsat 7 ETM+	2009-09-18	166/062	Visible & NIR	30 m
Landsat 8 OLI	2014-03-25	166/062	Visible & NIR	30 m
Landsat 8 OLI	2016-12-27	166/062	Visible & NIR	30 m
Landsat 8 OLI	2018-04-05	166/062	Visible & NIR	30 m
Landsat 8 OLI	2020-04-26	166/062	Visible & NIR	30 m
Landsat 8 OLI	2021-03-01	166/062	Visible & NIR	30 m

used in this work. It is worth noting that due to the challenge of cloud cover the study could not find many images.

2.3. Satellite Image Preprocessing. Satellite sensor data typically contains unique radiometric and geometric errors, necessitating rectification. Due to differences in scene illumination and viewing geometry, atmospheric correction, and sensor noise, radiometric correction was required. Each of the mentioned conditions varies depending on the sensors used to collect the data and the conditions at the time of data collection. Furthermore, data calibration was required as a preprocessing operation to convert digital values to known (absolute) radiation or reflectance measurements in order to simplify data comparability. The goal of pre-processing is to improve image data by suppressing undesired distortion and enhancing certain visual properties that are useful for subsequent processing [29]. Despite the fact that many sensor data (e.g. MODIS) come in handy with atmospheric correction already done, some sensors like Landsat TM/ETM+ lack this advantage; hence calling for atmospheric correction. This correction includes Rayleigh scattering, gaseous absorption, and aerosol scattering in the VIS channels (480 nm, 560 nm, 660 nm) and NIR channels 830 nm (H. Quaidran,1998).

The FLAASH module in ENVI 5.3 software based on MODTRAN 4 Radiative Transfer model was used to convert Landsat-7 ETM+ sensor to surface reflectance [30]. MODTRAN will change digital numbers (DN) into radiance. Moreover, it does not only convert DN into reflectance but also remove effect of atmosphere. The above preprocessing procedures were done also to Landsat 5. To enhance compatibility of Landsat 5,7 and 8 their Visible and Near- infrared bands were layer stacked and resampled to target resolution.

Finally, images were reprojected to ensure the downloaded images conform to world reference system. This enhanced compatibility with Arc-GIS mapping.

3. Image Classification

3.1. Data Training. Maximum likelihood algorithm demands that image data must be trained by the user before classification. The "seeds" picked by the analyst; either from the image or from study area forms the basis of assignment to classes of the highest probability. For effective training one must first determine the number of land cover types in the study area therefore, prior information of the study area is a pre-requisite [31]. The challenge of class separation can be addressed by measuring the class separability of the chosen training pixels; the Jeffries-Matusita (JM) distance can be used. For normally distributed classes JM separability for two classes, J_{ij} is defined in equation (1).

$$J_{ij} = \sqrt{2(1 - e^{-\alpha})} \quad (1)$$

Where α is Bhattacharyya distance.

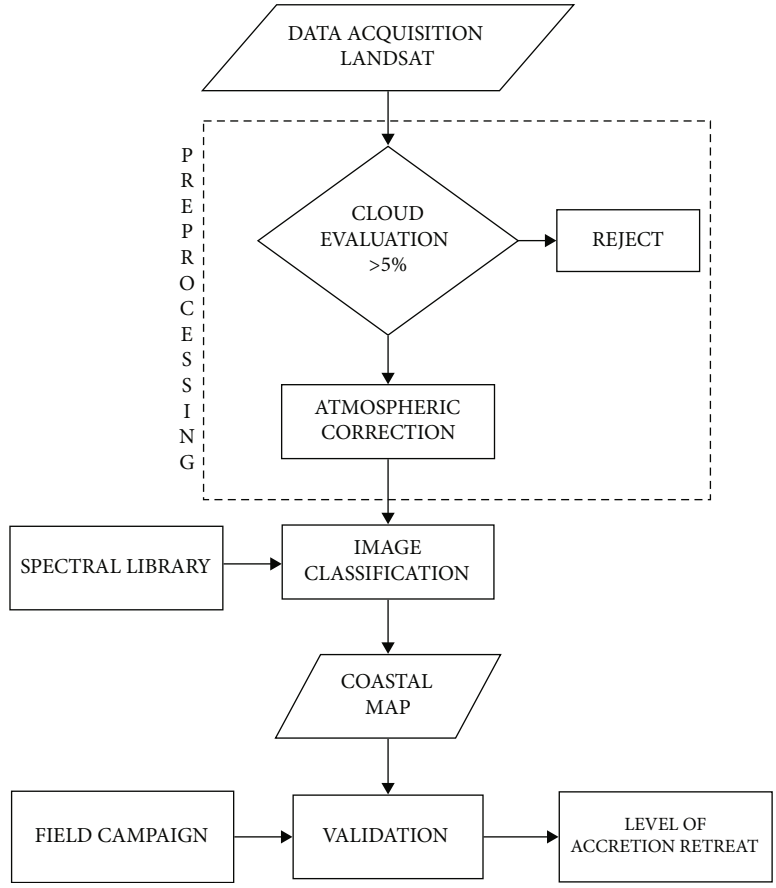

Figure 3: Flow chart showing image preprocessing, processing and validation procedures.

J_{ij} ranges from 0 to 2.0, $J_{ij}>1.9$ implies good separability of classes, for moderate separability the range is $1.0 \leq J_{ij} \geq 1.90$ and poor separability for $J_{ij} < 1.0$.

On ENVI 5.3 software the pre-processed image was loaded and locations utilized as training sites for each land cover class were established. Google Earth software with most recent photos of the affected area was loaded side by side with intention of identifying possible number of classes in the study area. With ROI subset technique areas covered with each endmember was picked and saved in endmember collection library. The training care was taken to ensure that picking was done at the center of a particular endmember. This reduced considerably the chances of possible error during classification. The saved endmembers ROI were later used in classification.

3.2. Classification of the Images. Data retrieved from ROIs ("seeds") are the determinant of good classification and mapping of ecological systems such as; morphodynamics, forests and wetlands. Regions with various endmembers tend to have ROIs with complex heterogeneous system [32]. In this study we classified the pixels of the Landsat images as mangrove, bare land, water, shrubs, and settlement using a supervised maximum likelihood (MLC) technique. These techniques assume that (1) a continuous set of ground features relevant to the investigation can be separated into discrete categories, and (2) those categories can be mapped using satellite data ([31].). Background knowledge of the research region derived from external sources or field activity is required for supervised classification. Masking out the study area was done mainly to avoid cloudy area.

In this study, we adopted a per-pixel technique. Image classification and accuracy assessment were undertaken after mangrove, barren ground, shrubs, water, and settlement sample and classification were scaled relative to pixel size. The Region of Interest (ROI) of the spectral signatures of the individual endmembers was used to classify the remote sensing image of the study area. The ENVI 5.3 interface module high probability threshold for each class was set for best input. The probabilities were computed by changing the input values between 0.1 and 1.0 to get the best results. The processes outlined in Figure 3 highlights the overall steps required in mapping the evolution of the coastline in this research area.

3.3. Validation. Field campaign was conducted in the study area. We navigated to the location using GCPs loaded in our GPS gadget. Using GPS machine, the location for each endmember was taken by standing at the center of approximately 30x30 m area of each endmember. The sample of points picked were loaded on ENVI 5.3 platform and used to reclassify the area based on new findings. By comparing initially

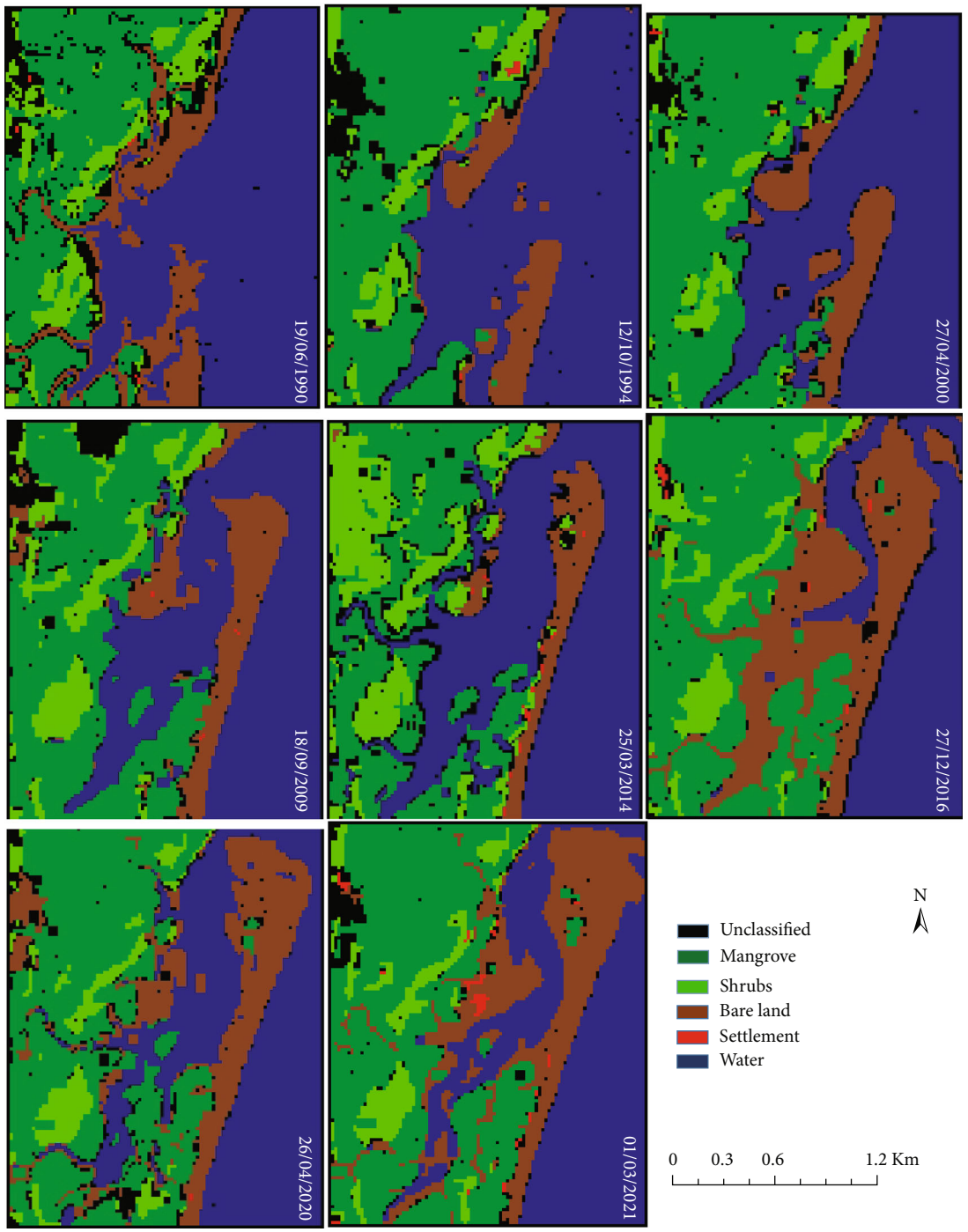

Figure 4: The temporal trend of endmembers from 1990 to 2021.

classified and newly classified, confusion matrix was generated. Equation (2) shows accuracy assessment formula

$$\text{Overall accuracy}(\text{OA}) = \frac{N_{AA} + N_{BB} + N_{CC}}{N} x\,100\% \quad (2)$$

Where N is the total number of points and N_{AA}, N_{BB}…..N_{ZZ} are endmembers correctly classified (sum of elements in main diagonal of the confusion matrix).

4. Results and Discussion

4.1. Classification Results. Remote sensing and GIS techniques were used to track the changing coastline along Kadzuyuni beach (Mto Tamamba region) in Kenya's North coast. Comparing multi-temporal remote sensing imagery with aid of ENVI and GIS shows temporal coastal change (areas of erosion and accretion) from 1990 to 2021. Figure 4 illustrates a combination of erosion and accretion places along the Mto Tamamba area. The vast majority of

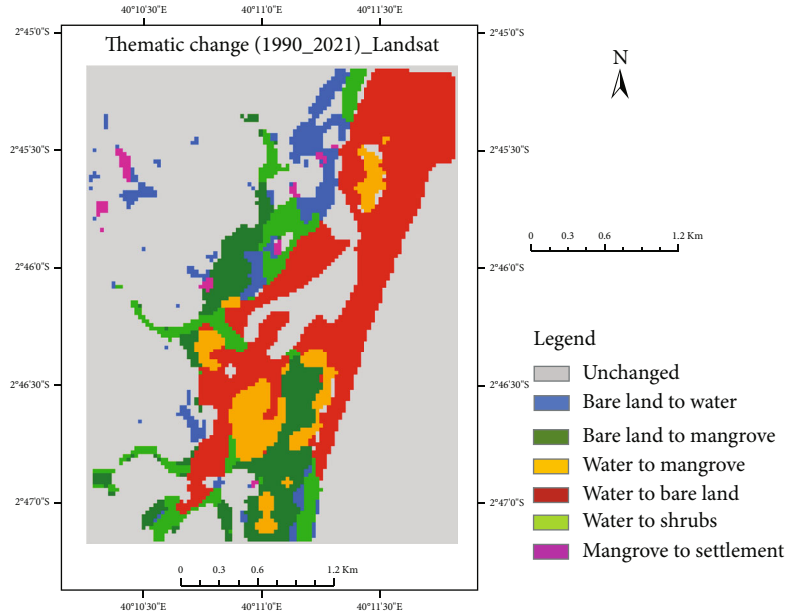

Figure 5: Thematic change in the study area between 1990-2021.

Table 3: Confusion matrix for the Landsat data.

Class	Water_1	Mangrove_1	Shrubs_1	Bare land_1	Settlement_1	User Total
Water	9	0	0	2	0	11
Mangrove	1	8	0	0	0	9
Shrubs	0	2	10	0	0	12
Bare land	1	0	0	9	2	12
Settlement	0	0	0	0	6	6
Producer Total	11	10	10	11	8	50

changes are as a result of naturally occurring processes during this study period. The findings show that majority of the coastline along the Mto Tamamba delta has been prograding. This is supported by the fact that pixel area of the class bare land is seen prograding in the areas initially occupied by endmember water. In fact, some vegetation is observed to have grown on the advanced areas. It is also observed that such advancement has been occurring progressively over time and space.

Ground truthing exercise done on this area confirms that; the contributor to this threat is the regular flooding of ocean waters into the land (a common feature of coastal beaches), to which Kenya is not immune. On a daily basis, water dynamics in the form of waves sweep the ocean bed and erode the sediments onshore. When water returns to the ocean, it does so gradually, leaving behind silt that contributes to accretion. The sediments left behind are rich in dead micro-organisms, which promote mangrove germination. Most settlements in this area are temporary structures which are built by fishermen who migrate depending on availability of fish. Because there has been little development, mangroves have been able to establish themselves well providing strong line of defense thereby avoiding land loss.

Table 4: Results of confusion matrix.

Confusion matrix
Overall accuracy = (42/50) 84.00%
Kappa coefficient =0.7989

4.2. Thematic Change between 1990 and 2021. The results show that there was erosion and prograding in the studied area throughout the period of this study. There was an overall increase in bare land, indicating that top alluvial soil had been pushed downstream over time as shown in Figure 5.

The red part of the image depicts an increase in bare land inside water surrounding Mto Tamamba. The dark green emphasizes places that have transitioned from bare land to mangrove throughout the years, while the orange highlights areas that have transitioned from water to Mangrove over the 31-year period. A ground truthing operation was done to confirm the desktop application with an overall accuracy of 84% and kappa coefficient of 0.799 as shown in Table 3.

4.3. Accuracy Assessment. Data collected from the field trip using GPS device was used to reclassify the study area with

Table 5: Change detection statistics 1990-2021.

		Landsat change detection statistics (1990 and 2021) Area per pixel count Initial Stage-1990						
		Unclassified	Water	Mangrove	Shrubs	Bare land	Settlements	Total raw
Final Stage-2021	Unclassified	603	65	20	99	60	3	850
	Water	163	3235	35	126	224	0	3783
	Mangrove	483	552	2868	127	584	0	4614
	Shrubs	94	0	108	535	23	6	766
	Bare land	116	1835	21	23	486	1	2482
	Settlements	14	19	0	14	31	0	78
	Class total	1473	5706	3052	924	1408	10	
	Class changes	870	2471	184	389	922	10	
	Image difference	-623	-1923	1562	-158	1074	68	

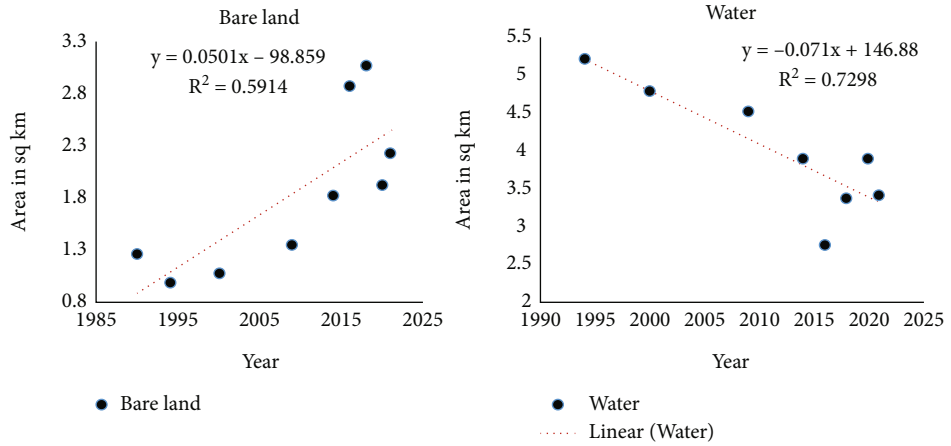

Figure 6: Time series plots for bare land and water.

intention of validating the supervised classification results initially obtained. The confusion matrix gave overall accuracy of 84% and kappa coefficient of 0.799 as shown in Table 4. Overall accuracy formula used in ENVI 5.3 is explained in equation (2).

4.4. Change Detection Statistics between 1990 and 2021. The change data were calculated using ENVI 5.3 software during the two periods (1990-2021). The change statistics were produced to depict the movement of the coastline through time for a land/seaward area from the existing coastline. According to Table 5, there was a total decrease by water body of 1923 pixels over the 31-year period. Over these years, the area covered by mangrove expanded by 1562 pixel counts. The endmembers bare land and settlement also registered an increment of pixel counts of 1074 and 68 respectively. The increase in bare land confirms the reason for prograding land as seen by the satellite. From this observation we conclude that bare land prograding into the ocean reduces the pixel count area of endmember water. Field campaign done in this area ascertains that an increase in mangroves in the study region is due to silt eroded downstream by Mto (river) Tamamba. The silt provides a conducive environment for the establishment of vegetation. The economic activities of the people living in this region is primarily fish farming. These fishermen relocate regularly in quest for better fishing grounds. People are also being relocated as a result of the area's desalination efforts.

4.5. Time Evolution of Endmembers. Pixel area of coverage for each endmember was plotted against time using excel software (Figure 6). The endmembers bare land and water exhibit positive and negative linear regression, with $R^2 = 0.5914$ and $R^2 = 0.7298$ respectively. This suggests that there is a gradual decrease of the pixel area covered by water bodies over time owing to the fact that some of its initial area was covered by bare land.

4.6. Spatial Correlation of the Endmembers. When plotted on a graph using Excel software, the statistics for endmembers water and bare land gave a negative correlation, with $R^2 = 0.5138$ as shown in Figure 7 below. Endmembers bare land and mangrove on the other hand, have a positive correlation of $R^2 = 0.468$. We conclude from this correlation plots that an increase in bare land towards the ocean results in a decrease in the area of pixels initially occupied by water. The fact that land is seen prograding towards the ocean is an indication that sediment is pilling in this region. The

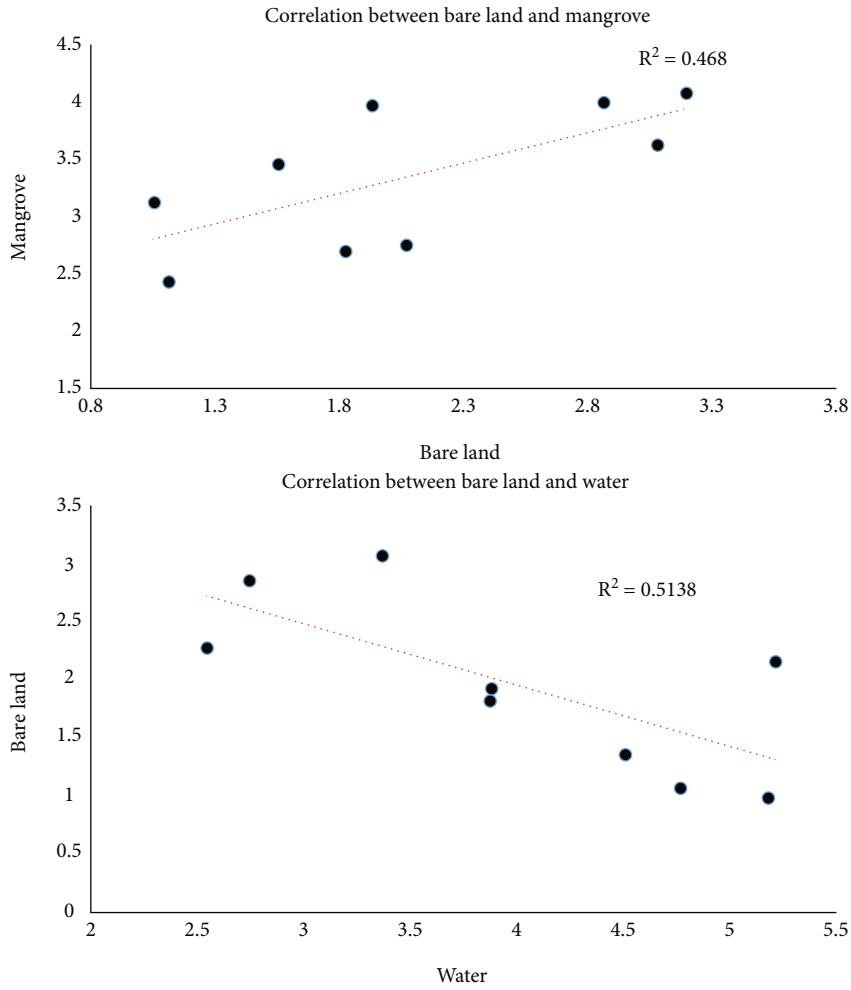

Figure 7: Correlation graphs comparing relation of endmembers in the Landsat data.

vegetation and bare land have a favorable link because eroded soil contains fertile alluvial deposit, which encourages the growth of sparse and dense vegetation such as mangrove forest [33]. It should be noted that in this region, water is advancing into the land on a daily basis between noon and 6 p.m. This water advancement facilitates dispersion of mangrove seedling into the land. This water gradually returns back in the Ocean from midnight leaving sediments behind. These eventually leads to evolution of the coastline.

4.7. Discussion. The study of Kenyan coastline evolution using remote sensing and GIS techniques has provided realistic information about the state of evolution. This is supported by comparing the results from two sets of data shown in Figure 8 (1990 and 2021, respectively). The fact that the outcome reveals a land prograding North-Eastwards inside the Ocean, suggests that the objective of using thematic change and time-series technique to monitor and map evolution of coastline was successful. Further details reveal that endmembers mangrove, shrubs and some settlements are slowly creeping on the new area; an indication that the process of evolution has been long to warrant the growth of vegetation and support life of ecosystem. Field campaign confirms the participation of erosion and influence of water dynamics as key contributors of this menace. The change in land-sea interface due to natural and human influence has clearly been depicted in this outcome [34]. Indeed, the participation of erosion and water dynamics have dramatically changed the shape of Kenyan coastline. The accuracy of the results produced from the ground truthing exercise was 84%. The figure reveals an expansion of coastline mainly towards the ocean. With minimal recession of land along the coastline.

Figure 9 shows graphical presentation of pixel area coverage for each endmember in the study area for 1990 and 2021 respectively. It can be deduced from the figure that pixel area for water has reduced over the 31-year period under investigation. Whereas the pixel area for bare land has increased. This is an indication that the land is eating up areas initially covered by water pixels. The main cause being erosion of both Mto Tamamba bed and hydrodynamic effect.

With different degrees of effectiveness, Landsat satellite imageries have been employed in the past and in recent years in a range of coastal applications, including monitoring of shoreline alterations [3, 14, 15, 34–36]. Despite the availability of a variety of high-resolution imageries, Landsat satellite images remain the most essential remote sensing

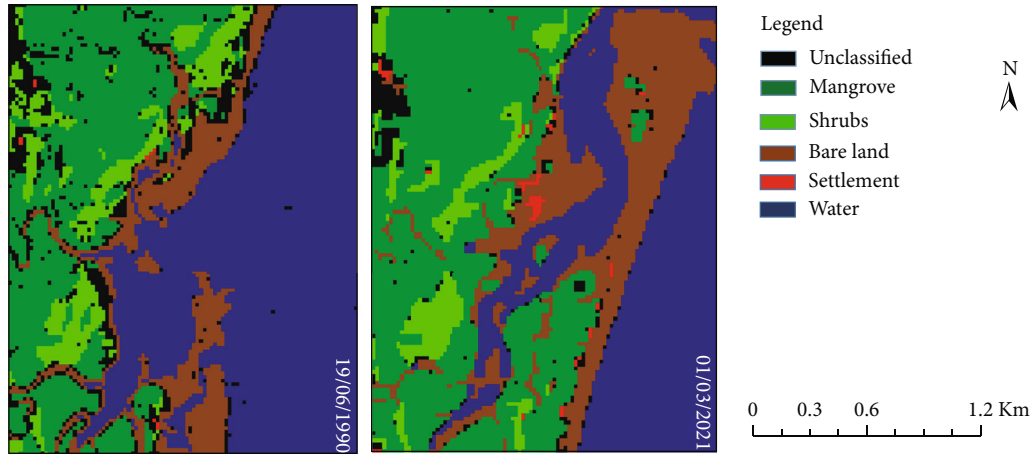

Figure 8: Classified images for Mto Tamamba area for 1990 and 2021, respectively.

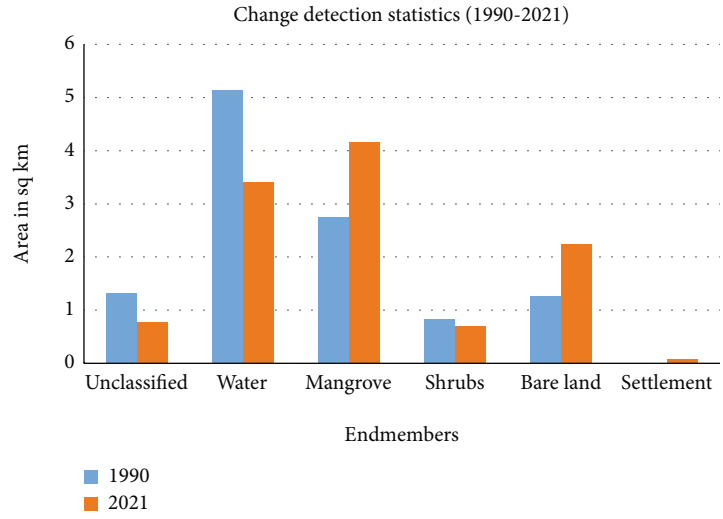

Figure 9: Comparison of classified endmembers based on pixel area coverage for the two years, respectively.

data for monitoring changes because of its' advantage of earlier launch and free data acquisition. Its application in Kenyan coast has yield a positive result.

The climate at the Kenyan coast is tropical humid therefore the challenge of cloud cover is obvious. This challenge has made many researchers avoid using satellite data. This study provides, to the best of our knowledge the first application of RS and GIS in monitoring Kenyan coastline. In this study, coastline change has been visualized and analyzed consistently through time and space. With extraction of endmember pixel area statistics, time series trend for each endmember has been established. The output provides a powerful new insight into pattern and process of coastal morphology by significantly showing coastline change that could not easily be achieved by field survey.

Ground truthing exercise establishes that the main cause of this evolution is among others erosion of Tamamba river bed as well as hydrodynamic effect on the seabed; another contributing factor is daily recession of Indian Ocean water (negative serge) that floods the land carrying along with it dead aqua micro-organisms [37]. These micro-organisms decompose providing conducive environment for growth of vegetation (shrubs and mangroves). The accuracy of the results produced from the ground truthing exercise was 84%. Field observation further confirms that areas with mangrove forest were less affected with erosion and accretion. This is because mangrove which are self-maintaining and naturally growing trees act as line of defense against water tides and human activities. Mangroves contribute goods and services to coastal ecosystem that are of economical, ecological and environmental importance. Such ecosystem services, prevent the coastline and farms against erosion [38]. Erosion associated with deforestation, poor agricultural practice and dredging of seabed is prevalent at the Kenyan coast [22]. As a result, mangroves provide better and cheaper coastal protection than man-made engineering buildings along a shoreline.

One of the most visible effects of climate change is accelerated sea level rise. Sea level increases at a rate of 1.3 mm per year along Indian coasts, according to [39]. Rising sea levels wreak havoc on the coast, causing a plethora of erosional hazards. The depth of the water, as well as the depth of the wave base, increases as the sea level rises. As the waves

reach the shoreline, their intensity increases, allowing them to erode and transport more sediment. As a result, the water level begins to rise along the coast. Tidal waves, storm surges, and flooding are all enhanced by rising sea levels. These effects are harmful not only to coastal ecosystems (mangroves, turtles that deposit their eggs on the sand) but also to coastal constructions. The findings from the analysis show that the Kenyan coast underwent all these changes within the time period studied.

Coastal erosion has negative impact on agriculture thereby affecting food production. Besides, the breeding ground for marine ecosystem is interfered with. Tourist industry, the second largest foreign exchange earner in Kenya faces risk as many jobs are lost due lack of space for structural erection of beach hotels [40]. Furthermore, foreign investors willing to invest at the coast require background information about coastal erosion before making right decision on structural investments. This research can be used as a database for local governments and the federal government when making decisions about coastal zone management.

5. Conclusion and Recommendations

The objective of this study was determining the temporal shoreline changes along the Kenyan coastline using remote sensing and GIS. The extent and magnitude of the coastal erosion and accretion which occurred were used to identify priority areas and suggest suitable preventive measures. The study of Kenyan coastline evolution using remote sensing and GIS techniques has provided insight into problems and challenges brought by coastal erosion. This suggests that this method can successfully be used for mapping and monitoring coastal changes. The accuracy of the results produced from the ground truthing exercise was 84%. The fact that multi-spatial and multi-temporal time scale changes can be achieved using RS and GIS makes us conclude that this technique is a powerful tool of monitoring soil erosion and evolution of coastline.

RS and GIS information have very great significance in terms of planning of coastal zones. Moreover, the application of these technologies would aid in the development of a robust mapping project and provide greater clarity on erosion risk areas for both public and private entities. Secondly, information from such findings can be used by developers in making sound decision on where to erect coastal structures to prevent effects of land recession or plant more mangrove tree for defense. Thirdly, statistical findings can be used to create applied cartography of risk areas, such as maps of susceptible and vulnerable geo-hazards. Based on current findings we recommend that Kenyan government should build structured walls along the coastline in land receding areas. Alternatively, more mangrove trees should be planted to minimize effect of tidal wave along the coastline. However, it should be noted that images of higher-resolution like IKONOS, SPOT and Sentinel-2 may provide better alternative to this work by showing changes on the ground in greater details. Finally, future researchers should make full use of this technology and incorporate it into their studies of coastline change.

Data Availability

The data shall be available upon request from the corresponding author.

Conflicts of Interest

The authors declare that they have no conflicts of interest.

Acknowledgments

The author is indebted to Department of Physics University of Nairobi who directly or indirectly supported him in the progress of his research work towards its successful completion. The author acknowledges the University of Nairobi for scholarship award. The study was funded by the University of Nairobi Department of Physics masters scholarship.

References

[1] A. Mukhopadhyay, S. Mukherjee, S. Mukherjee, S. Ghosh, S. Hazra, and D. Mitra, "Automatic shoreline detection and future prediction: a case study on Puri coast, bay of Bengal, India," *European Journal of Remote Sensing*, vol. 45, no. 1, pp. 201–213, 2012.

[2] D. Kong, C. Miao, A. G. L. Borthwick et al., "Evolution of the Yellow River Delta and its relationship with runoff and sediment load from 1983 to 2011," *Journal of Hydrology*, vol. 520, pp. 157–167, 2015.

[3] M. Latella, A. Luijendijk, A. M. Moreno-Rodenas, and C. Camporeale, "Satellite image processing for the coarse-scale investigation of Sandy coastal areas," *Remote Sensing*, vol. 13, no. 22, p. 4613, 2021.

[4] S. Maiti and A. K. Bhattacharya, "Shoreline change analysis and its application to prediction: a remote sensing and statistics based approach," *Marine Geology*, vol. 257, no. 1–4, pp. 11–23, 2009.

[5] E. C. F. Bird, *Coastal Geomorphology: An Introduction*, John Wiley & Sons, 2011.

[6] S. Saravanan, N. Chandrasekar, M. Rajamanickam, C. Hentry, and V. Joevivek, "Management of Coastal Erosion Using Remote Sensing and GIS techniques (SE India)," *The International Journal of Ocean and Climate Systems*, vol. 5, no. 4, pp. 211–221, 2014.

[7] W. de Boer, Y. Mao, G. Hagenaars, S. de Vries, J. Slinger, and T. Vellinga, "Mapping the Sandy Beach evolution around seaports at the scale of the African continent," *Journal of Marine Science and Engineering*, vol. 7, no. 5, p. 151, 2019.

[8] M. R. Phillips and A. L. Jones, "Erosion and tourism infrastructure in the coastal zone: problems, consequences and management," *Tourism Management*, vol. 27, no. 3, pp. 517–524, 2006.

[9] W. Chaib, M. Guerfi, and Y. Hemdane, "Evaluation of coastal vulnerability and exposure to erosion and submersion risks in Bou Ismail Bay (Algeria) using the coastal risk index (CRI)," *Arabian Journal of Geosciences*, vol. 13, no. 11, p. 420, 2020.

[10] I. Burton, B. Lim, E. Spanger-Siegfried, E. L. Malone, and S. Huq, *Adaptation Policy Frameworks for Climate Change: Developing Strategies, Policies, and Measures*, Cambridge University Press, 2005.

[11] R. N. Jones, "An Environmental Risk Assessment/Management Framework for Climate Change Impact Assessments," *Natural hazards*, vol. 23, no. 2, pp. 197–230, 2001.

[12] F. Leone, F. Lavigne, R. Paris, J.-C. Denain, and F. Vinet, "A spatial analysis of the December 26th, 2004 tsunami-induced damages: lessons learned for a better risk assessment integrating buildings vulnerability," *Applied Geography*, vol. 31, no. 1, pp. 363–375, 2011.

[13] R. Mani Murali, M. Ankita, S. Amrita, and P. Vethamony, "Coastal vulnerability assessment of Puducherry coast, India, using the analytical hierarchical process," *Natural Hazards and Earth System Sciences*, vol. 13, no. 12, pp. 3291–3311, 2013.

[14] X.-Z. Wang, H.-G. Zhang, B. Fu, and A. Shi, "Analysis on the coastline change and erosion-accretion evolution of the Pearl River estuary, China, based on remote-sensing images and nautical charts," *Journal of Applied Remote Sensing*, vol. 7, no. 1, article 073519, 2013.

[15] K. White and H. M. El Asmar, "Monitoring changing position of coastlines using thematic mapper imagery, an example from the Nile Delta," *Geomorphology*, vol. 29, no. 1–2, pp. 93–105, 1999.

[16] M. A. K. Elsayed and S. M. Mahmoud, "Groins system for shoreline stabilization on the east side of the Rosetta promontory, Nile Delta coast," *Journal of Coastal Research*, vol. 232, pp. 380–387, 2007.

[17] L. Cenci, C. Santella, G. Laneve, and V. Boccia, "(PDF) evaluating the potentialities of Copernicus very high resolution (VHR) optical datasets for assessing the shoreline erosion Hazard in microtidal environments," 2021, https://www.researchgate.net/publication/354577120_Evaluating_the_Potentialities_of_Copernicus_Very_High_Resolution_VHR_Optical_Datasets_for_Assessing_the_Shoreline_Erosion_Hazard_in_Microtidal_Environments.

[18] R. S. Sridhar, K. Elangovan, and P. K. Suresh, "Long term shoreline oscillation and changes of Cauvery Delta coastline inferred from satellite imageries," *Journal of Sustainable Development*, vol. 2, no. 1, p. 132, 2009.

[19] Ş. Şener, E. Şener, B. Nas, and R. Karagüzel, "Combining AHP with GIS for landfill site selection: a case study in the Lake Beyşehir catchment area (Konya, Turkey)," *Waste Management*, vol. 30, no. 11, pp. 2037–2046, 2010.

[20] T. Kuleli, A. Guneroglu, F. Karsli, and M. Dihkan, "Automatic detection of shoreline change on coastal Ramsar wetlands of Turkey," *Ocean Engineering*, vol. 38, no. 10, pp. 1141–1149, 2011.

[21] T. M. Munyao, "Environmental effects of Coastal Sedimentation: A Case study fo Shirazi-Funzi Lagoon," 1993, http://www.oceandocs.org/handle/1834/334.

[22] E. Odada, "Contribution of Africa's coastal and marine sectors to sustainable development," 2001, https://aquadocs.org/handle/1834/7009.

[23] U. K. Johnson, "River sediment supply, sedimentation and transport of the highly turbid sediment plume in Malindi Bay, Kenya," *Journal of Geographical Sciences*, vol. 23, no. 3, pp. 465–489, 2013.

[24] J. C. Hoorweg and N. Muthiga, *Advances in coastal ecology: people, processes and ecosystems in Kenya*, African Studies Centre, Leiden, Netherlands, 2009.

[25] C. A. Omuombo, D. O. Olago, and E. O. Odada, "Coastal Erosion," in *Developments in Earth Surface Processes*, P. Paron, D. O. Olago, and C. T. Omuto, Eds., pp. 331–339, Elsevier, 2013.

[26] P. A. Abuodha, *Effects Of Shoreline Change On Sandy Beach Environments Of Malindi—Mambrui area, northern Kenyan Coast*, Kenya Marine and Fisheries Research Institute, 2003.

[27] P. Camberlin and O. Planchon, "Coastal precipitation regimes in kenya," *Physical Geography*, vol. 79, no. 1-2, pp. 109–119, 1997.

[28] A. Latawiec and D. Agol, *Sustainability indicators in practice*, De Gruyter Open Poland, 2015.

[29] N. E. Young, R. S. Anderson, S. M. Chignell, A. G. Vorster, R. Lawrence, and P. H. Evangelista, "A survival guide to Landsat preprocessing," *Ecology*, vol. 98, no. 4, pp. 920–932, 2017.

[30] "Getting Started with ENVI Tutorial," 2022, August 5, 2022, https://www.l3harrisgeospatial.com/docs/gettingstartedwithenvitutorial.html.

[31] A. Ahmad and S. Quegan, "Analysis of Maximum Likelihood Classification on Multispectral Data," *Applied Mathematical Sciences*, vol. 6, no. 129, pp. 6425–6436, 2012.

[32] T. M. Berhane, H. Costa, C. R. Lane, O. A. Anenkhonov, V. V. Chepinoga, and B. C. Autrey, "The influence of region of interest heterogeneity on classification accuracy in wetland systems," *Remote Sensing*, vol. 11, no. 5, p. 551, 2019.

[33] G. T. Ayele, A. Kuriqi, M. A. Jemberrie et al., "Sediment yield and reservoir sedimentation in highly dynamic watersheds: the case of Koga Reservoir, Ethiopia," *Water*, vol. 13, no. 23, p. 3374, 2021.

[34] M. Kostiuk and M. Geography, "Using remote sensing data to Detect Sea level change," *International Archives of Photogrammetry Remote Sensing and Spatial Information Sciences*, vol. 34, no. 1, pp. 105–113, 2002.

[35] M. A. Azab and A. M. Noor, "Change Detection of the North Sinai Coast by Using Remote Sensing and Geographic Information System," in *The 4th International Conference and Exhibition for Environmental Technologies Environment*, pp. 1102–1111, Egypt, 2003.

[36] L. Changming and Z. Shifeng, "Drying up of the yellow river: its impacts and counter-measures," *Mitigation and Adaptation Strategies for Global Change*, vol. 7, no. 3, pp. 203–214, 2002.

[37] J. MacDonald, *When the Sea Recedes*, JSTOR Daily, 2017, https://daily.jstor.org/when-the-sea-recedes/.

[38] P. A. W. Abuodha and J. G. Kairo, "Human-induced stresses on mangrove swamps along the Kenyan coast," *Hydrobiologia*, vol. 458, no. 1, pp. 255–265, 2001.

[39] J. A. Church, P. U. Clark, A. Cazenave et al., "Sea-level rise by 2100," *Science*, vol. 342, no. 6165, pp. 1445–1445, 2013.

[40] J. S. Akama and D. Kieti, "Tourism and socio-economic development in developing countries: a case study of Mombasa resort in Kenya," *Journal of Sustainable Tourism*, vol. 15, no. 6, pp. 735–748, 2007.